

1 **Komatiites Constrain Molybdenum Isotope Composition of the Earth's Mantle**

2

3 Nicolas D. Greber<sup>1,\*</sup>, Igor S. Puchtel<sup>2</sup>, Thomas F. Nägler<sup>1</sup>, and Klaus Mezger<sup>1</sup>

4

5 *<sup>1</sup>Institute of Geological Sciences, University of Bern, Baltzerstrasse 3, CH-3012 Bern; Tel: +41 31*  
6 *631 8533*

7 *<sup>2</sup>Department of Geology, University of Maryland, College Park, Maryland 20742, USA, Tel: (301)*  
8 *405-4054*

9 *<sup>+</sup>Present address: Origins Laboratory, Department of the Geophysical Sciences, The University of*  
10 *Chicago, 5734 South Ellis Avenue, Chicago, IL 60637, USA*

11

12 *\*Corresponding author. E-mail: greber@uchicago.edu*

13

14 **Abstract**

15 In order to estimate the Mo isotopic composition and Mo abundance in the Bulk Silicate Earth  
16 (BSE), a total of thirty komatiite samples from five localities on three continents were analyzed using  
17 an isotope dilution double spike technique. Calculated Mo concentrations of the emplaced komatiite  
18 lavas range from  $25 \pm 3$  to  $66 \pm 22$  ng/g, and the inferred Mo concentrations in the deep mantle  
19 sources of the komatiites range between  $17 \pm 4$  and  $30 \pm 12$  ng/g, with an average value of  $23 \pm 7$   
20 ng/g (2SE). This average value represents our best estimate for the Mo concentration in the BSE; it is  
21 identical, within the uncertainty, to published previous estimates of  $39 \pm 16$  ng/g, but is at least a factor  
22 of 2 more precise.

23 The Mo isotope compositions of the komatiite mantle sources overlap within uncertainty and  
24 range from  $\delta^{98}\text{Mo} = -0.04 \pm 0.28$  to  $0.11 \pm 0.10$  ‰, with an average of  $0.04 \pm 0.06$  ‰ (2SE). This value  
25 is analytically indistinguishable from published Mo isotope compositions of ordinary and enstatite  
26 chondrites and represents the best estimate for the Mo isotopic composition of the BSE. The inferred  
27  $\delta^{98}\text{Mo}$  for the BSE is therefore lighter than the suggested average of the upper continental crust (0.3 to  
28 0.4 ‰). Thus, from the mass balance standpoint, a reservoir with lighter Mo isotope composition  
29 should exist in the Earth's mantle; this reservoir can potentially be found in subducted oceanic crust.

30 The similarity of Mo isotopic compositions between chondritic meteorites and estimates for the  
31 BSE from this study indicates that during the last major equilibration between Earth's core and mantle,  
32 i.e., the one that occurred during the giant impact that produced the Moon, chemical and isotopic  
33 equilibrium of Mo between Fe metal of the core and the silicate mantle was largely achieved.

34

35 Keywords: Mo isotopic composition, komatiites, Bulk Silicate Earth, chondritic meteorites,  
36 core-mantle equilibrium

37

## 38 1. Introduction

39 Molybdenum is a redox-sensitive element with a refractory and moderately siderophile  
40 character, and, as such, is well suited for studies of chemical differentiation of the Earth ranging from  
41 core-mantle differentiation to low temperatures surface processes. Mass-dependent fractionation of  
42 stable Mo isotopes has been used for modeling core formation temperatures (Hin et al., 2013;  
43 Burkhardt et al., 2014), reconstruction of the extent of past ocean euxinia (e.g., Arnoldt et al. 2004,  
44 Pearce et al., 2008; Baldwin et al., 2013) and constraining the timing of the onset of Earth's  
45 atmosphere oxygenation (e.g., Wille et al., 2007).

46 The interpretation of Mo isotopes and their variations in different terrestrial reservoirs is limited  
47 by the lack of knowledge of the Mo isotope composition of the Bulk Silicate Earth (BSE). This value is  
48 difficult to determine because Mo isotopes can fractionate significantly during magmatic and post-  
49 magmatic processes (Voegelin et al, 2014; Greber et al., 2014). Voegelin et al. (2014) showed that  
50 amphibole and biotite crystallizing from a silicate melt are enriched in light Mo with  
51  $\Delta^{98}\text{Mo}_{\text{melt-mineral}} \geq 0.5 \text{ ‰}$ . Furthermore, combined LA-ICP-MS studies and leaching experiments of  
52 basalts indicate that magmatic sulfides have on average a higher Mo concentration and a heavier  
53  $\delta^{98}\text{Mo}$  than the bulk rock (Voegelin et al., 2012). Thus, even at high-temperatures, Mo isotope  
54 fractionation can cause substantial  $\delta^{98}\text{Mo}$  heterogeneity within a terrestrial reservoir. Based on the  
55 analyses of molybdenites (Greber et al., 2014) and the Mo isotopic data available for igneous  
56 continental crustal rocks, an average  $\delta^{98}\text{Mo}$  value of 0.3 to 0.4 ‰ is inferred for the Earth's igneous  
57 continental crust (Voegelin et al., 2014). While recently published  $\delta^{98}\text{Mo}$  values for ordinary, enstatite  
58 and most carbonaceous chondrites, as well as iron meteorites, show a homogenous  $\delta^{98}\text{Mo}$  of  
59  $0.09 \pm 0.02 \text{ ‰}$  (95% confidence interval; n=12), achondrites generally have heavier Mo isotope  
60 compositions (Burkhardt et al., 2014). This is consistent with the experimental data suggesting  
61 significant Mo isotope fractionation between liquid metal and liquid silicate up to  $\sim 2500^\circ\text{C}$ , where the  
62 lighter Mo isotopes preferentially enter the metal phase (Hin et al., 2013). On the basis of the Mo  
63 isotopic data for chondritic meteorites, Burkhardt et al. (2014) estimated the  $\delta^{98}\text{Mo}$  for the BSE  
64 between 0.09 and 0.25 ‰. However, direct determinations of the Mo isotope composition of the  
65 Earth's mantle have so far not been available.

66 In this study, komatiites from five different localities from around the globe were investigated in  
67 order to better constrain the Mo abundances and Mo isotopic composition of the Archean mantle.

68 Komatiites are particularly appropriate for this type of study because they are high-MgO volcanic rocks  
69 that formed by high degrees of partial melting (~30 to 50%; Arndt, 1977) of the mantle. This melting  
70 regime commonly leads to the sampling of large mantle domains, the complete base metal sulfide  
71 removal from the residual mantle and the production of sulfur-undersaturated melts (e.g., Keays,  
72 1995). This results in an almost quantitative removal of Mo from the source into the melt and it is  
73 therefore expected that the Mo isotope composition of komatiite melts represent the composition of  
74 their melting source regions. Komatiite lavas erupted at temperatures of up to 1600°C (Nisbet et al.,  
75 1993), which further limits potential Mo isotope fractionation.

76

## 77 **2. Samples**

78 A total of thirty komatiite samples from five localities were investigated. Three sample sets come  
79 from the Barberton Greenstone Belt in South Africa, and were collected from the lower and upper  
80 Komati and the Weltevreden Formations. The upper Komati samples show strong alteration features  
81 and were selected to study the effects of alteration on the Mo isotopic systematics. The fourth set  
82 comes from the Pyke Hill area in the Abitibi Greenstone Belt (Canada). The fifth set is from the  
83 Vetreny Belt in Fennoscandia.

84 The samples from the different locations represent several chemical types of komatiites that  
85 derived from mantle source regions characterized by variable degrees of depletion/enrichment. Those  
86 from the lower Komati Formation have Barberton-type  $Al_2O_3/TiO_2$  ratios of around 10; their primitive  
87 mantle-normalized REE abundance patterns show slight enrichments in light REE and strong  
88 depletions in heavy REE (Puchtel et al., 2013). The studied Weltevreden komatiites belong to the Al-  
89 enriched type (Connolly et al., 2011) and have primitive mantle-normalized REE patterns exhibiting  
90 depletions in light REE and enrichments in heavy REE (Puchtel et al., 2013). The Pyke Hill komatiites  
91 belong to the Munro type lavas with  $Al_2O_3/TiO_2 \sim 20$ . Their primitive mantle normalized REE patterns  
92 show depletions in light REE and essentially flat heavy REE abundances (Puchtel et al., 2004b). The  
93 komatiites from Victoria's Lava Lake have REE patterns showing enrichment in LREE, which is  
94 interpreted to be the result of contamination of the initially LREE-depleted komatiite magma with upper  
95 crustal rocks (Puchtel et al., 1996, Puchtel et al., 1997). In order to evaluate the effects of crustal  
96 contamination, two tonalite samples (K04, K13) from the Vodla Block, consisting of early Archean

97 tonalite-trondhjemite-granodiorite complexes thought to underlie the Vetreny Belt lavas (Puchtel et al.,  
98 1997), were also analyzed for their Mo concentrations and isotopic compositions.

99 More information about the samples is given in the Supplementary Material and an overview of  
100 sampling details is presented in Table 1.

101

### 102 **3. Analytical techniques**

#### 103 **3.1. Mo isotope and concentration measurements**

104 For this study, lower Komati Formation and Weltevreden komatiite sample powders prepared by  
105 Puchtel et al. (2014), Pyke Hill sample powders from the Puchtel et al. (2004a and 2004b) studies, and  
106 the Victoria's Lava Lake and tonalite sample powders from Puchtel et al. (2015) were used. The  
107 details of the sample powder preparation techniques are reported in the cited publications. For the  
108 upper Komati Formation samples from Tjakastad, altered surfaces were cut off with a diamond saw.  
109 The rest of the rock was then cut into small pieces and powdered in an agate disk mill.

110 Depending on the Mo concentration of the sample, between 0.6 and 2.6 g of material was  
111 weighed out into Savillex<sup>®</sup> PFA beakers and spiked with a <sup>100</sup>Mo-<sup>97</sup>Mo double spike. Samples were  
112 initially digested for one day in a 5:1 mixture of 22.6 M HF and 14.4 M HNO<sub>3</sub> at room temperature.  
113 Then, the sample-acid mixtures were heated in closed beakers to 110°C for ca. 3 days with repeated  
114 treatment in an ultrasonic bath. Subsequently they were dried down at 110°C and re-dissolved at  
115 130°C in a 2:1 mixture of 6.4 M HCl and 14.4 M HNO<sub>3</sub> for several days and then dried down again.  
116 After this treatment, only chromites were not digested; these chromites were separated from some  
117 samples and used for further analyses by LA-ICP-MS. In preparation for the ion exchange  
118 chromatography, the solutions were converted into the chloride form via re-dissolution in 6.4 M HCl  
119 and drying down again. Molybdenum was then separated from the matrix with a sequential procedure  
120 involving anion and cation exchange chromatography, as described by Wille et al. (2007). Depending  
121 on the amount of sample material used, more than one anion exchange column step was necessary  
122 and each sample was therefore dissolved in the corresponding amount of HCl-H<sub>2</sub>O<sub>2</sub>. These steps  
123 sometimes produced a gel and therefore it was necessary to centrifuge the samples prior to Mo  
124 separation. After the anion column chemistry, only one cation exchange chromatography step was

125 needed to obtain a clean Mo cut. The total analytical blank for Mo was 2 to 3 ng, which corresponds to  
126 2 to 10% of total Mo processed. For several samples (e.g. PH31, 564-5, BV15), however, the blank  
127 contribution was as high as 15%. Therefore, 19 out of the 32 samples were replicated with more  
128 sample material processed to decrease the blank/sample ratio (up to 80% less blank). All but one  
129 analysis (sample BV13) reproduced within analytical uncertainties. In addition, no trend towards  
130 heavier or lighter  $\delta^{98}\text{Mo}$  values was observed as a function of blank/sample ratios (see Figure S1).  
131 Therefore, a strongly fractionated Mo isotope composition of the blank contribution, which would be  
132 needed to shift the measured  $\delta^{98}\text{Mo}$  values, can be excluded.

133 The  $\delta^{98}\text{Mo}$  compositions were analyzed using a double focusing Nu Instruments<sup>TM</sup> MC-ICP-MS  
134 system. The use of a double-spike allowed for the simultaneous determination of the Mo isotope  
135 composition and the Mo concentration. Mass-spectrometry routine and double spike calibration are  
136 described in detail in Greber et al. (2012). The Mo isotope composition is conventionally given as  
137  $\delta^{98}\text{Mo}$  notation:

$$138 \quad \delta^{98}\text{Mo} = \left( \frac{{}^{98}\text{Mo}/{}^{95}\text{Mo}_{\text{sample}}}{{}^{98}\text{Mo}/{}^{95}\text{Mo}_{\text{reference}}} - 1 \right) \cdot 1000 \quad (1)$$

139 The data are normalized using the conventional techniques outlined in Nägler et al. (2014), e.g.,  
140 the  $\delta^{98}\text{Mo}$  of NIST SRM 3134 is equal to +0.25 ‰ and mean ocean water has a Mo isotope  
141 composition of  $2.34 \pm 0.07$  ‰. This standardization will be used for the discussion throughout this  
142 study.

143 Komatiites have high Ru concentrations, an element that has natural isotopes that have isobaric  
144 interferences with  ${}^{100}\text{Mo}$  and  ${}^{98}\text{Mo}$ . Ruthenium was not completely removed by the Mo chemistry and,  
145 therefore, corrections for isobaric interferences were applied based on the monitored intensity of the  
146  ${}^{99}\text{Ru}$  peak. More information on the Ru correction,  ${}^{99}\text{Ru}$  signal and  ${}^{99}\text{Ru}/{}^{95}\text{Mo}$  ratios can be found in the  
147 supplementary material and Table S1 and Figure S2. External precision of standard reference material  
148 measurements (NIST SRM 3134 and 610, and NIST SRM 612 glasses) was better than  $\pm 0.10$  ‰  
149 (2SD; see Greber et al., 2012) and represents the true uncertainty on the measured Mo isotopic ratios,  
150 unless stated otherwise. The USGS rock standard SDO-1 processed and analyzed during the same  
151 analytical campaign yielded an average  $\delta^{98}\text{Mo} = 1.07 \pm 0.05$  ‰ (2SD, n=5), which is in agreement with  
152 the suggested value of  $1.05 \pm 0.14$  ‰ (Goldberg et al., 2013).

153

### 154 **3.2. LA-ICP-MS; bulk rock chemistry and chromites**

155 Major and trace element concentrations of the two strongly altered Tjakastad samples were  
156 determined by XRF and LA-ICP-MS on  $\text{Li}_2\text{B}_4\text{O}_7$  glasses. XRF measurements were performed on an  
157 Axios, PANalytical wavelength-dispersive X-ray fluorescence spectrometer at the Institute of  
158 Geochemistry and Petrology, Department of Earth Sciences, ETH Zürich, Switzerland. LA-ICP-MS  
159 was done using an ELAN DRCE quadrupole mass spectrometer (QMS; Perkin Elmer, Canada)  
160 coupled with a pulsed 193 nm ArF Excimer laser (Lambda Physik, Germany) and an energy-  
161 homogenized (Microlas, Germany) beam profile. Details on the setup and optimization strategies can  
162 be found in Pettke et al. (2012). The chromite residua from the sample digestion were collected,  
163 placed on thin section slides and chromite grains larger than 40  $\mu\text{m}$  were analyzed using LA-ICP-MS.

## 164

### 165 **4. Results**

166 Molybdenum concentrations and Mo isotopic compositions of the studied komatiite and tonalite  
167 samples are presented in Table 1.

168 The Mo concentrations of the komatiites from the lower Komati Formation range from 13 to  
169 51 ng/g and the  $\delta^{98}\text{Mo}$  values range from  $0.11 \pm 0.10$  to  $0.69 \pm 0.10$  ‰. The  $\delta^{98}\text{Mo}$  and the Mo  
170 concentrations correlate well with each other and with the indices of magmatic differentiation (Figures  
171 1A, 2 and 3). The Mo concentrations correlate negatively with elements compatible in olivine, such as  
172 MgO and Ni (Figures 1A and 2D), and positively with the incompatible elements, such as  $\text{Al}_2\text{O}_3$  and  
173  $\text{TiO}_2$  (Figure 2A and 2B). The  $\delta^{98}\text{Mo}$  values show negative correlations with the Mo concentrations  
174 and positive with the MgO concentrations (Figure 3). Molybdenum concentrations correlate with Pt  
175 (Figure 2C) and Pd. The sample from the chilled margin (BV02) has the highest Mo concentration and  
176 the lightest  $\delta^{98}\text{Mo}$ ,  $\sim 0.18$  ‰ lighter than the olivine cumulate from the same lava flow (BV01).

177 The Mo concentrations of the samples from the Weltevreden Formation range from 9 to 30 ng/g.  
178 The Mo isotope compositions range from  $-0.04 \pm 0.10$  to  $0.13 \pm 0.10$  ‰ (Figure 4). The Mo  
179 concentration of the lava flows SA501 and KBA12 correlate negatively with MgO (Figure 1B) and Ni  
180 (Figure 2D) and positively with the elements that are incompatible in olivine (e.g.  $\text{Al}_2\text{O}_3$ ,  $\text{TiO}_2$ , Pt, see  
181 Figure 2). The only two samples from flow SA564 analyzed (i.e. 564-4 and 564-5) have lower Mo  
182 concentrations that plot below these trends (see Figures 1B and 2), which may indicate Mo mobility

183 during postmagmatic processes. This is at odds with the Re behavior in these samples, which shows  
184 no evidence for disturbance (Connolly et al., 2011; Puchtel et al., 2014).

185 The Mo concentrations of the samples from the Pyke Hill komatiites range from 18 to 46 ng/g  
186 and show the same correlations with geochemical parameters as observed in the other two komatiite  
187 locations. The  $\delta^{98}\text{Mo}$  values span a very narrow range between  $-0.07 \pm 0.10 \text{ ‰}$  and  $0.17 \pm 0.10 \text{ ‰}$   
188 (Figure 4) and do not correlate with other geochemical parameters.

189 The Mo concentrations of the Victoria's Lava Lake samples are the highest among the studied  
190 komatiites and range from 114 to 256 ng/g. The  $\delta^{98}\text{Mo}$  values range between  $0.06 \pm 0.10$  and  
191  $0.32 \pm 0.10 \text{ ‰}$ . There is no correlation between the Mo isotope composition and the lithology within the  
192 lava lake or any available geochemical data. The Mo concentrations exhibit, as expected, negative  
193 correlations with elements compatible in olivine (Figures 1E and 2D) and positive correlations with  
194 incompatible elements (Figures 2A and 2B).

195 The two analyzed Tjakastad samples from the upper Komati Formation have high  $\text{SiO}_2$ ,  $\text{Na}_2\text{O}$ ,  
196  $\text{Al}_2\text{O}_3$  and low MgO and Ni concentrations, indicating that these rocks were strongly altered. The Mo  
197 isotope compositions and Mo concentrations are similar in both samples, at around  $0.70 \text{ ‰}$  and 81  
198 ng/g, respectively. Major and trace element concentrations of these samples are given in Table S2.

199

## 200 **5. Discussion**

### 201 **5.1. General considerations**

#### 202 **5.1.1. Chromites**

203 Due to their high resistance to acid attack, chromites were not completely digested during the  
204 chemical procedures applied, which potentially resulted in an analytical bias in determining the Mo  
205 isotopic composition and concentration in the samples. In order to evaluate the effect of undigested  
206 chromites on the bulk rock Mo concentration and isotope composition, chromites from several  
207 komatiite samples were analyzed for their Mo concentration by LA-ICP-MS. The major element  
208 compositions of these chromites were also analyzed and are reported in Table S3; these are similar to  
209 those reported in Puchtel et al. (1996). The Mo concentrations in the chromites determined by LA-ICP-  
210 MS are below the detection limit, except for some chromite grains in sample 91111 from Victoria's  
211 Lava Lake. Calculating a Mo partition coefficient ( $K_d$ ) based on the Mo concentration in sample 91111  
212 gives a  $K_{d\text{chromite-melt}} = 11$ . Using this value and an assumption that all Cr in the sample is present in



213 chromite, it is calculated that the Mo contribution of the chromites to the total Mo inventory in the bulk  
214 rock is less than 5%. This value can be considered a maximum estimate, and was likely much less,  
215 since there are also other minerals in the studied samples that contain Cr, such as olivine and  
216 orthopyroxene. Although olivine is not a major host of Cr ( $K_{d_{Ol-melt}}$  for Cr is around 0.7: Adam and  
217 Green 2006), orthopyroxene is ( $K_{d_{Opx-melt}}$  around 8: Adam and Green 2006). Based on these  
218 considerations, we conclude that the undigested chromites likely had a negligible effect on the  
219 measured bulk rock Mo isotope compositions and concentrations.

220

### 221 **5.1.2. Alteration and magmatic Mo isotope fractionation**

222 Since Mo species are soluble in water under oxidizing conditions, Mo might have been  
223 mobilized during secondary alteration. Thus, it is essential to consider the influence of alteration  
224 processes on the Mo isotope composition and concentrations. A commonly used technique to  
225 evaluate mobility of an element in komatiitic rocks is to plot this element against indices of magmatic  
226 differentiation, such as MgO content, and evaluate if its abundances plot on olivine control lines (Arndt  
227 et al., 1977). This approach uses the fact that the only major liquidus phase in komatiitic magmas over  
228 a wide range of temperatures and pressures is olivine (Arndt, 1976). This approach is shown in Figure  
229 1 for the samples investigated here. If Mo concentrations were unaffected by secondary alteration, the  
230 olivine control line drawn through the Mo vs. MgO data should intersect the MgO-axis at the average  
231 MgO concentration of the olivine in equilibrium with the emplaced komatiite lava.

232 Here, we used the published MgO concentrations in olivines from the studied komatiite suites.  
233 The MgO vs. Mo regression line for Victoria's Lava Lake intersects the MgO-axis close to the average  
234 MgO content of the liquidus olivine in this system (i.e., ~48 wt.%, Puchtel et al., 1996), demonstrating  
235 immobile behavior of Mo during secondary alteration of this komatiite suite (Figure 1E).

236 For the Weltevreden komatiite suite, when omitting samples from lava flow SA564 (i.e., 564-4  
237 and 564-5), the regression line through the other samples intersects the horizontal axis at the MgO  
238 concentration of olivine from that locality (i.e., ~54 wt.%, Puchtel et al., 2013; Figure 1B). This  
239 suggests pristine Mo signatures for rock samples of lava flows SA501 and KBA12, but potentially  
240 lower Mo content in the samples from lava flow SA564 due to alteration. As there is no obvious  
241 difference in the Mo isotope composition between flow SA564 and the other two flows, the  $\delta^{98}\text{Mo}$   
242 seems to be unaffected by the alteration process at this locality.

243 The Mo concentrations of the Pyke Hill komatiite samples show a good correlation with the MgO  
244 content; however, samples plot on a regression line with a slope that is steeper than that of the olivine  
245 control line, indicating some Mo mobility in the cumulate samples, in-line with the observation of some  
246 limited mobility of Re in the same cumulate samples (Puchtel et al., 2004b). Nonetheless, all Pyke Hill  
247 komatiites have very similar and consistent  $\delta^{98}\text{Mo}$  values indicating that alteration processes affected  
248 Mo in the Pyke Hill samples only to a small degree, if at all. Regressions using the samples with the  
249 highest (PH14) and lowest (PH13) Mo concentration through the pre-defined olivine MgO  
250 concentration of ~52 wt% (Puchtel et al., 2004a) are used to calculate the concentrations of Mo in the  
251 emplaced komatiite lava and the mantle source of the Pyke Hill komatiites (Figures 1C-D).

252 The lower Komati Formation komatiites are the samples showing the biggest range in their Mo  
253 isotope compositions within the same locality (see Figure 3 and 4). Even though these rocks are well  
254 preserved by Archean standards, they were still modified by seafloor alteration and metamorphism  
255 (Puchtel et al., 2013). Although Mo concentrations show a good correlation with the MgO content, the  
256 data plot on a trend with a slope steeper than that of olivine control line (Figure 1A). This implies either  
257 (a) mobile behavior of Mo during seafloor alteration and/or metamorphism or (b) Mo concentrations  
258 and  $\delta^{98}\text{Mo}$  were influenced by magmatic fractionation or mantle source heterogeneity.

259 If alteration or metamorphism were significant, these processes have to account for the  
260 observation that the lower Komati Formation is the only studied location that exhibits significant Mo  
261 isotope variations and in addition, a correlation between the  $\delta^{98}\text{Mo}$  and MgO concentration. The  
262 heaviest  $\delta^{98}\text{Mo}$  of the lower Komati Formation (BV15 =  $0.69 \pm 0.10$  ‰) is similar to the Mo isotope  
263 composition of the strongly altered and geographically closely related Tjakastad samples from the  
264 upper Komati Formation (average of  $0.70 \pm 0.10$  ‰; Figure 4 and Table 1). This similarity might  
265 indicate that the Mo isotope compositions of the lower Komati samples are modified by alteration,  
266 whereby the samples with the lowest Mo concentrations are affected the most. A Mo isotope shift  
267 towards a heavier composition is in line with the observations about the behavior of Cr isotopes during  
268 weathering of ultramafic rocks (Farkaš et al., 2013). Even though Cr is not necessarily concentrated in  
269 the same minerals as Mo, both are redox sensitive elements, soluble under oxidizing conditions, and  
270 they form similar complexes under Eh and pH conditions of surface waters (i.e.  $\text{MoO}_4^{2-}$ ,  $\text{HMoO}_4^-$ ,  
271  $\text{H}_2\text{MoO}_4$  vs.  $\text{CrO}_4^{2-}$ ,  $\text{HCrO}_4^-$ ; Oze et al., 2007). Thus, Cr can serve as the first order analogue for Mo in  
272 these environments and during surface alteration of ultramafic rocks. Puchtel et al. (2014) provided

273 evidence that Re was mobile during alteration in these ultramafic rocks. This led to significant scatter  
274 in a Re vs. MgO diagram. As Re behaves geochemically similar to Mo, the striking correlation between  
275 Mo concentrations and  $\delta^{98}\text{Mo}$  with, e.g., MgO contents (Figure 3) is inconsistent with the suggestion  
276 that the Mo signature was modified by alteration. It rather indicates that the Mo concentrations  
277 obtained for these samples are most likely primary. If alteration or metamorphism cannot account for  
278 the variability of the Mo isotopes in the komatiites of the Komati Formation, then magmatic processes  
279 need to be considered.

280 High temperature Mo isotope fractionation in magmatic and hydrothermal systems has been  
281 observed and described in the literature, as has been outlined in the introduction. Silicate minerals,  
282 such as amphibole and biotite, have been shown to preferentially incorporate lighter Mo isotopes  
283 during crystallization in subduction-related magma chambers (Voegelin et al., 2014), leaving behind a  
284 melt enriched in isotopically heavy Mo. In addition, combined LA-ICP-MS measurements and leaching  
285 experiments of basalts revealed compatible behavior of Mo in early magmatic sulfide melt inclusions  
286 that are also hosts for heavier Mo isotopes (Voegelin et al., 2012). If igneous processes dominated the  
287 Mo signatures of the lower Komati Formation, the observed Mo concentrations and isotope  
288 compositions, as well as major and trace element compositions of these rocks, should show  
289 predictable trends.

290 Since Mo isotope compositions are heavier in samples with higher MgO concentrations (early  
291 precipitates), this implies that an early cumulate phase should have incorporated Mo with a  $\delta^{98}\text{Mo}$   
292 heavier than that of the melt. Silicate minerals, however, are inferred to incorporate lighter Mo  
293 isotopes, at least in systems with higher oxygen fugacity, a parameter that can influence the  
294 speciation of Mo and other elements and thus has an effect on the isotope fractionation of redox  
295 sensitive elements in general (see Dauphas et al., 2014). The V partitioning behavior between olivine  
296 and komatiite melt in the lavas from the lower Komati Formation and Weltevreden Formation indicates  
297 that these two komatiite systems differentiated under similar  $f\text{O}_2$  (Puchtel et al., 2013); however, their  
298 range of Mo isotope fractionations is different. This observation is inconsistent with  $f\text{O}_2$  being the  
299 dominant factor of Mo isotope fractionation in these rocks. Fractionation of sulfide minerals or  
300 immiscible sulfide liquid cannot explain the observed pattern either. The main argument against this  
301 possibility is that highly siderophile elements, such as Pt and Pd, that have a stronger affinity for  
302 sulfide phases than Mo, plot on olivine control lines (Puchtel et al., 2014) and, therefore, do not show

303 any evidence for fractionation of significant amounts of sulfides. In addition, experimentally determined  
304 Mo partition coefficients between sulfide phases and silicate liquid indicate that small amounts of  
305 sulfides do not strongly influence the Mo concentration of the silicate melt (Li and Audétat, 2012). Not  
306 much is known about the partitioning behavior of Mo in oxides. Chromite is the most common oxide  
307 phase fractionating in komatiite lavas when the MgO content of the liquid drops below 24% (Barnes,  
308 1998). However, Cr<sub>2</sub>O<sub>3</sub> concentrations in the samples from the lower Komati formation differ only by ±  
309 0.03 wt. %. Since chromites contain between 50 and 60 wt% Cr<sub>2</sub>O<sub>3</sub> (Table S3), only ca. 0.06%  
310 chromite is needed to account for the differences in the Cr concentrations among the samples. This  
311 small amount of chromite cannot account for the observed variations in the Mo isotopic compositions,  
312 unless the Mo partition coefficient between chromite and silicate melt is significantly higher compared  
313 to those obtained for the Weltevreden and Victoria's Lava Lake suites.

314 Another hypothesis would be that the Mo isotope fractionation occurred just after komatiite lava  
315 emplacement, but prior to its solidification. Samples BV01 and BV02 are from the same lava flow.  
316 Even though their δ<sup>98</sup>Mo are within error identical, the olivine cumulate sample BV01 follows closely  
317 the trend for the other cumulates towards a heavier δ<sup>98</sup>Mo. Sample BV02 is likely to be the one that  
318 best represents the primary lava compositions, because it is a chilled margin sample and, as such,  
319 had not experienced any substantial fractional crystallization. On this basis, an olivine control line can  
320 be drawn through the composition of this sample and that of the earliest olivine precipitates. Using this  
321 olivine control line, the deviation between the Mo concentrations of the samples and those predicted  
322 can be calculated for each analyzed sample. Using a Rayleigh distillation model, a very homogeneous  
323 δ<sup>98</sup>Mo fractionation of -0.41 ± 0.03 ‰ (2SD) can be estimated and a perfect fit through all data points  
324 is achieved (see Figure 5 and Table S4). This result indicates that the initial lavas from all flows could  
325 have been almost identical in their Mo concentrations and isotope compositions. A process during lava  
326 emplacement removing light Mo isotopes prior to crystallization of the komatiite rocks thus might  
327 account for the observed isotope variations and the steeper Mo vs MgO trend. The fractionating phase  
328 could be a Mo bearing mineral or metal alloy that was sequestered right after lava emplacement and  
329 was not sampled by the rocks investigated.

330 Alternative causes for the correlation of Mo isotopes with higher MgO could be mantle source  
331 heterogeneity and/or dynamic melting during the ascent of a plume, similar to what has been  
332 suggested for the Gorgona komatiites (Arndt et al., 1997). Indeed, Puchtel et al. (2013) argued for a

333 decrease in trace element concentrations in the studied komatiite lava flows from the bottom of the  
334 lava sequence upwards, which caused steepening of the MgO vs trace element trends when samples  
335 from across the lava sequence were plotted together. Both, mantle source heterogeneity or  
336 observation that succeeding komatiite lava flows were generated from progressively more depleted  
337 mantle domains within the same rising mantle plume, could account for the fractionated Mo signature  
338 of the lower Komati Formation komatiites. In this latter model, depletion of the lower Komati Formation  
339 mantle source results in lower Mo content but enrichment of heavy isotopes. The strength of this  
340 hypothesis is that it explains the steep Mo vs. MgO trend, the good correlation between  $\delta^{98}\text{Mo}$  and  
341 MgO, as well as the decrease in other trace element concentrations from the bottom of the lava  
342 sequence upwards observed by Puchtel et al. (2013).

343 At this stage, no conclusive answer can be given as to which of the processes was most likely  
344 responsible for the observed Mo signature in the lower Komati Formation samples. Regardless of the  
345 specific mechanism that was responsible for the variations in the Mo isotopic compositions of the  
346 Komati lavas, chilled margin sample BV02 represents best the Mo isotopic composition of the  
347 emplaced komatiite lavas. Therefore, further calculations and interpretations regarding this komatiite  
348 suite will use the data for this sample only.

349

## 350 **5.2. Molybdenum concentrations and isotope compositions of the komatiite lavas**

351 The Mo concentration of the emplaced komatiite lavas can be estimated from the MgO vs. Mo  
352 regressions for samples from a given locality and using the published calculated MgO content of the  
353 emplaced komatiite lava from Puchtel et al., (1996), Puchtel et al., (2004a), Connolly et al. (2011) and  
354 Puchtel et al., (2013). The MgO concentrations of the emplaced lavas at the lower Komati and  
355 Weltevreden Formation komatiites are  $29.4 \pm 0.3$  wt. % and  $31.4 \pm 0.9$  wt. %, respectively (Connolly et  
356 al. 2011, Puchtel et al., 2013). The MgO concentration of the primary komatiite lava at Pyke Hill has  
357 been shown to be 27.4 wt. % (Puchtel et al. 2004a). The emplaced komatiite lava at Victoria's Lava  
358 Lake had a MgO concentration of 14.8 wt. % (Puchtel et al., 1996). The calculated primary Mo  
359 concentrations of the emplaced komatiite lavas, using either olivine control lines or fitted regressions,  
360 are  $33 \pm 8$  ng/g for Pyke Hill,  $25 \pm 4$  ng/g for Weltevreden, and  $51 \pm 6$  ng/g for the lower Komati  
361 locality.

362 For the Weltevreden and lower Komati Formations, an estimated uncertainty on the regression  
363 was used to calculate the maximum and minimum Mo concentrations at the limits of the MgO  
364 concentrations of the emplaced komatiite lava (see Figure 1). The estimated error on the primary Mo  
365 concentration of the lower Komati Formation is  $\pm 5$  ng/g, resulting from a 10% uncertainty on the Mo  
366 concentration of sample BV02. The error on the primary Mo concentration of the emplaced komatiite  
367 lava at the Weltevreden locality has been defined using the error estimate on the Mo concentration  
368 from the MgO vs. Mo regression, i.e.,  $\pm 2.5$  ng/g. For the Pyke Hill komatiites, a maximum (sample  
369 PH14) and minimum (sample PH31) regression through the pre-defined MgO concentration of olivine  
370 were used to estimate the uncertainties (Figure 1).

371 The original komatiite melt from Victoria's Lava Lake assimilated around 8% of crustal material  
372 *en route* to the surface (Puchtel et al., 1996). Since the material of the continental crust is estimated to  
373 contain ca. 800 ng/g Mo (Rudnick and Gao, 2003), crustal contamination must have resulted in the  
374 increase in Mo concentrations in the emplaced Vetreny komatiite lava. In order to calculate the Mo  
375 content in the original Vetreny komatiite magma, the contribution from the crustal contaminant first  
376 needs to be accounted for. Two tonalites from the Vodla block, which were expected to represent the  
377 contaminant, were analyzed for their Mo concentrations and isotope compositions. The Mo  
378 concentrations of the tonalites range from 15 to 46 ng/g (Table 1), which is even lower than those  
379 obtained for the Victoria's Lava Lake komatiites. This implies that either this particular samples lost a  
380 substantial amount of their Mo inventory after emplacement of the komatiites, or that these samples  
381 are not representative for the composition of the contaminant in terms of their Mo content. Therefore,  
382 the estimated Mo content of the bulk continental crust of 800 ng/g (Rudnick and Gao 2003) is used to  
383 account for the effects of crustal contamination. Based on the well-defined MgO vs. Mo correlations in  
384 the Vetreny lava lake, the contaminated komatiite lava upon emplacement is calculated to contain  
385  $175 \pm 18$  ng/g Mo. To account for the effects of olivine fractionation prior to lava emplacement, the Mo  
386 concentration in the inferred original komatiite lava with  $25 \pm 2.5$  wt% MgO (Puchtel et al., 1996) was  
387 calculated using the composition of the actual emplaced komatiite lava with 14.8% MgO and  $175 \pm 18$   
388 ng/g Mo and the estimated liquidus olivine composition with 50 wt.% MgO in equilibrium with the  
389 original komatiite (Puchtel et al., 1996). This results in a Mo concentration of  $125 \pm 18$  ng/g for a  
390 komatiite lava with  $\sim 25$  wt% MgO. From this value, the effects of  $8 \pm 1\%$  crustal contamination were

391 subtracted, which yields a Mo content of  $66 \pm 22$  ng/g for the original, uncontaminated melt of the  
392 Victoria's Lava Lake komatiites.

393 The estimated 8% contamination with the continental crustal material results in  $62 \pm 13\%$  of the  
394 Mo inventory in the Victoria's Lava lake komatiite being derived from that of the contaminant. The  
395  $\delta^{98}\text{Mo}$  value of  $0.17 \pm 0.07$  ‰ obtained for the Victoria's lava lake komatiites is, therefore, dominated  
396 by the Mo isotopic composition of the contaminant. Although the Mo isotopic composition of the bulk  
397 continental crust has not yet been defined. Voegelin et al. (2014) suggested that the upper continental  
398 crust had a  $\delta^{98}\text{Mo}$  of around  $0.3 \pm 0.1$  ‰. As such, this value is used to account for the effect of crustal  
399 contamination on the Mo isotopic composition of the original komatiite magma. Our calculations yield  
400  $\delta^{98}\text{Mo}$  of  $-0.04 \pm 0.28$  ‰ for the uncontaminated Victoria's Lava Lake komatiite melt. For these  
401 calculations Monte Carlo simulation (20'000 cycles) was used for error propagation assuming a 10%  
402 uncertainty on the initial values where no error estimates have been available.

403

404 The very homogeneous  $\delta^{98}\text{Mo}$  values within the Victoria's Lava Lake, Pyke Hill and  
405 Weltevreden komatiite systems indicate that Mo isotope fractionation during differentiation of these  
406 komatiite lavas was very limited. The bulk Mo isotope composition of the komatiite lavas for each of  
407 the three localities can therefore be calculated as the average of the samples analyzed. Averaging  
408 ( $\pm 2\text{SE}$ ) yields  $\delta^{98}\text{Mo} = 0.05 \pm 0.06$  ‰ for Pyke Hill,  $0.04 \pm 0.04$  ‰ for Weltevreden and  $-0.04 \pm 0.28$  ‰  
409 for Victoria's Lava Lake. For the Komati locality, the  $\delta^{98}\text{Mo}$  of the chilled margin sample BV02 with  
410  $0.11 \pm 0.10$  ‰ (2SD of a single measurement) is used here as our best estimate for the Mo isotopic  
411 composition of the emplaced Komati lava.

412 Although determined with various degree of precision, the obtained Mo isotopic compositions for  
413 the four komatiite systems are identical within their respective uncertainties. Averaging Mo isotopic  
414 compositions for the four komatiite systems yields a  $\delta^{98}\text{Mo}$  of  $0.04 \pm 0.06$ ‰ (2SE, Table 2). This value  
415 represents our best estimate for the average Mo isotopic composition of the studied Archean  
416 komatiites.

417

### 418 **5.3. Molybdenum concentrations and isotope compositions of the komatiite** 419 **mantle sources**

420 The Mo concentrations in the mantle sources of the studied komatiite systems were estimated  
421 using the same projection technique utilized in this study for calculating the Mo concentration of the  
422 emplaced komatiite lava. This technique has been applied to calculate the absolute abundances of the  
423 incompatible highly siderophile elements (e.g., Pt, Pd, and Re) in the mantle sources of the Pyke Hill  
424 (Puchtel et al., 2004a), the lower Komati, and the Weltevreden Formation komatiites (Puchtel et al.,  
425 2014). The MgO content of the mantle is only influenced to a minor degree by previous melt  
426 extractions and thus, a MgO concentration from 38 to 40 wt%, similar to that in the Bulk Silicate Earth  
427 estimates of McDonough and Sun (1995), is assumed for the komatiite mantle sources. The errors  
428 were estimated in the same way as for the calculation of the Mo concentration in the emplaced  
429 komatiite lavas. Calculations give  $30 \pm 12$  ng/g for Victoria's Lava Lake,  $17 \pm 5$  ng/g for Pyke Hill,  $17 \pm$   
430  $3$  ng/g for Weltevreden, and  $29 \pm 7$  ng/g for the lower Komati Formation komatiite mantle sources.  
431 Averaging all four calculated values (Table 2) yields  $23 \pm 7$  ng/g (2SE), which is our best estimate for  
432 the BSE. This value is identical, within the uncertainties, to estimates for Mo concentration in the  
433 primitive mantle of  $39 \pm 16$  ng/g (Figure 6) calculated on the basis on an assumed constant Mo/Ce  
434 ratio of  $\sim 0.3$  (Palme and O'Neill, 2004).

435 Due to the high degrees of partial melting, the complete base metal sulfide removal from the  
436 mantle melting region, and the high liquidus temperatures of the komatiite lavas, it is assumed in this  
437 study that the  $\delta^{98}\text{Mo}$  values of the emplaced komatiite lavas closely resemble the Mo isotope  
438 compositions of their respective mantle sources. The average of Mo isotope compositions of the  
439 mantle sources of the studied komatiites is  $0.04 \pm 0.06$  ‰ (2SE); we consider this  $\delta^{98}\text{Mo}$  value as  
440 representing the Mo isotope composition of the Bulk Silicate Earth, as defined by the Mo isotopic  
441 composition of mantle sources of Archean komatiite systems. This value is indistinguishable from the  
442 chondritic  $\delta^{98}\text{Mo}$  value of  $0.09 \pm 0.02$  ‰ (Burkhardt et al., 2014) (Figures 2 and 6).

443 The calculated Mo isotopic composition of the BSE is lighter than the estimated average Mo  
444 isotopic composition ( $\delta^{98}\text{Mo} = 0.3$  to  $0.4$ ‰) of the upper igneous continental crust (Voegelin et al.,  
445 2014). From the mass-balance standpoint, an isotopically lighter reservoir compared to the BSE must  
446 exist in the Earth's mantle. This reservoir could be represented by subducting slabs that are expected  
447 to accumulate at either the transition zone, or even the core-mantle boundary (Kerr, 1997, Van der  
448 Hilst and Karason, 1999). Incorporation of the material of recycled oceanic crust in mantle plumes may  
449 result in lighter Mo isotope composition of some plume lavas.



450

#### 451 **5.4. Implications for the core-mantle equilibration**

452 It is assumed that late stages of Earth accretion involved collisions of several Moon- to Mars-  
453 sized planetary embryos, which were already differentiated into a metallic core and a silicate mantle  
454 (e.g., Wood et al., 2006, Stevenson 2008, Rudge et al., 2010). An open discussion exists as to the  
455 extent to which the metallic cores of the planetary embryos were equilibrated with the silicate liquid  
456 during and after the collisions. If the cores of the planetary embryos were dispersed as metal droplets  
457 after the impact, then they should have equilibrated with the silicate mantle at temperatures above  
458 2500°C (e.g., Wood et al., 2006; Siebert et al., 2013), which is the temperature at which Mo isotope  
459 fractionation between silicate and metal liquid becomes smaller than the current analytical precision of  
460 the Mo isotopic analysis (Hin et al., 2013). If Earth's core formed by merging of several metallic cores  
461 without complete equilibration with the silicate portion of the planet, then the Bulk Silicate Earth  $\delta^{98}\text{Mo}$   
462 should carry a memory of the core-forming events that happened in the planetary embryos, a process  
463 suggested to have occurred at lower temperatures (e.g., Kleine et al., 2009, Rudge et al., 2010 and  
464 Stevenson, 2008). That should result in Mo isotopic composition of the terrestrial mantle being distinct  
465 from that of the accreted chondritic material. Thus, the most straightforward interpretation of the  
466 similarity of Mo isotopic composition between chondritic meteorites, and estimates for the Bulk Silicate  
467 Earth from this study is that during the final stages of terrestrial accretion, metal droplets equilibrated  
468 with the silicate liquid and the chemical equilibrium between Fe metal of the core and the silicate  
469 mantle was essentially achieved.

470 The results of Mo partitioning experiments under various conditions allow elucidating the  
471 temperature and pressure at the time of Earth's core formation. Wade et al. (2012) proposed that the  
472 W and Mo composition of the BSE is best explained with sulfur addition during the last 10 to 20% of  
473 Earth's core formation. In contrast, based on Mo concentrations only, Burkemper et al. (2012)  
474 suggested that the pressures and temperatures during a single stage core forming event must have  
475 been between 40-54 GPa and 2775-3125°C (at  $f\text{O}_2 = -2.2 \Delta\text{IW}$  and using KLB-1 peridotite composition  
476 as a proxy for the silicate melt). This temperature is inline with a chondritic Mo isotope composition of  
477 the BSE.

478 The average chondritic Mo concentration of  $1332 \pm 430$  ng/g (2SD) (Burkhardt et al., 2014) is  
479 used to estimate the effect of the addition of late accreted materials constituting 0.5% of the terrestrial

480 mass (e.g. Mann et al., 2012) on the BSE's Mo inventory. Such an event would have resulted in the  
481 addition of  $6.7 \pm 2.0$  ng/g Mo to Earth's early mantle, which corresponds to around 17% or 29%,  
482 assuming a post accretion BSE Mo concentration of 39 ng/g (Palme and O'Neill 2004) or 23 ng/g (this  
483 study), respectively. Therefore, Mo addition via late accretion did not influence significantly the Mo  
484 isotope composition of a mantle with a near chondritic  $\delta^{98}\text{Mo}$ .

485 Further studies on Mo isotope fractionation during silicate liquid – metal liquid separation and  
486 the influence of sulfur, in combination with a more precisely defined  $\delta^{98}\text{Mo}$  of the Bulk Silicate Earth  
487 and chondritic meteorites might help better understand the conditions of core formation on Earth and  
488 other terrestrial planets.

489

## 490 **Acknowledgments**

491 Helen Williams and two unknown reviewers are thanked for their constructive criticism and Bernard  
492 Marty is thanked for the editorial handling. Provision of Komati and Weltevreden samples by Gary  
493 Byerly and Euan Nisbet to I.S.P. enabling us to use them in this study is gratefully acknowledged.  
494 Thomas Pettke is thanked for help with LA-ICP-MS measurements.

495

## 496 **References**

- 497 Adam, J. and Green, T., 2006, Trace element partitioning between mica- and amphibole-bearing garnet lherzolite  
498 and hydrous basanitic melt: 1. Experimental results and the investigation of controls on partitioning behaviour.  
499 Contributions to Mineralogy and Petrology 152: 1-17.
- 500 Arnold, G.L., Anbar, A.D., Barling, J., Lyons, T.W., 2004. Molybdenum isotope evidence for widespread anoxia in  
501 mid-Proterozoic oceans. Science 304, 87–90.
- 502 Arndt, N.T., 1976, Melting relations of ultramafic lavas (komatiites) at one atmosphere and high pressure: Year  
503 book - Carnegie Institution of Washington, 75, 555–562.
- 504 Arndt, N.T., 1977, Ultrabasic magmas and high-degree melting of the mantle. Contributions to Mineralogy and  
505 Petrology, v. 64, pp. 205-221
- 506 Arndt N.T., Naldrett A.J. and Pyke D.R., 1977, Komatiitic and iron-rich tholeiitic lavas of Munro Township,  
507 northeast Ontario: Journal of Petrology, 18, 319–369.
- 508 Arndt, N.T., Kerr, A.C., and Tarney, J., 1997, Dynamic melting in plume heads: the formation of Gorgona  
509 komatiites and basalts: Earth and Planetary Science Letters, v. 146, no. 1.

510 Baldwin, G.J., Nägler, T.F., Greber, N.D., Turner, E.C., and Kamber, B.S., 2013, Mo isotopic composition of the  
511 mid-Neoproterozoic ocean: An iron formation perspective: *Precambrian Research*, v. 230, p. 168–178.

512 Burkemper, L.K., Agee, C.B., and Garcia, K.A., 2012, Constraints on core formation from molybdenum solubility  
513 in silicate melts at high pressure: *Earth and Planetary Science Letters*, v. 335-336.

514 Burkhardt, C.N., Hin, R.C., Kleine, T., and Bourdon, B., 2014, Evidence for Mo isotope fractionation in the solar  
515 nebula and during planetary differentiation: *Earth and Planetary Science Letters*, v. 391, no. C, p. 201–211.

516 Connolly, B.D., Puchtel, I.S., Walker, R.J., Arevalo, R., Jr., Piccoli, P.M., Byerly, G., Robin-Popieul, C., and Arndt,  
517 N., 2011, Highly siderophile element systematics of the 3.3Ga Weltevreden komatiites, South Africa:  
518 Implications for early Earth history: *Earth and Planetary Science Letters*, v. 311, no. 3-4, p. 253–263.

519 Dauphas, N., Roskosz, M., Alp, E.E., Neuville, D.R., Hu, M.Y., Sio, C.K., Tissot, F.L.H., Zhao, J., Tissandier, L.,  
520 Médard, E., and Cordier, C., 2014, Magma redox and structural controls on iron isotope variations in Earth's  
521 mantle and crust: *Earth and Planetary Science Letters*, v. 398, no. C.

522 Farkaš, J., Chrastný, V., Novák, M., Čadkova, E., Pašava, J., Chakrabarti, R., Jacobsen, S.B., Ackerman, L., and  
523 Bullen, T.D., 2013, Chromium isotope variations ( $\delta^{53/52}\text{Cr}$ ) in mantle-derived sources and their weathering  
524 products: Implications for environmental studies and the evolution of  $\delta^{53/52}\text{Cr}$  in the Earth's mantle over  
525 geologic time: *Geochimica et Cosmochimica Acta*, v. 123, p. 74–92.

526 Goldberg, T., Gordon, G.W., Izon, G., Archer, C., Pearce, C.R., McManus, J., Anbar, A.D., and Rehkämper, M.,  
527 2013, Resolution of inter-laboratory discrepancies in Mo isotope data: an intercalibration: *Journal of Analytical*  
528 *Atomic Spectrometry*, doi: 10.1039/c3ja30375f.

529 Greber, N.D., Pettke, T., and Nägler, T.F., 2014, Magmatic–hydrothermal molybdenum isotope fractionation and  
530 its relevance to the igneous crustal signature: *Lithos*, v. 190-191, no. C, p. 104–110.

531 Greber, N.D., Siebert, C., Nägler, T.F., and Pettke, T., 2012,  $\delta^{98/95}\text{Mo}$  values and Molybdenum Concentration  
532 Data for NIST SRM 610, 612 and 3134: Towards a Common Protocol for Reporting Mo Data: *Geostandards*  
533 *and Geoanalytical Research*, v. 36, no. 3, p. 291–300.

534 Hin, R.C., Burkhardt, C.N., Schmidt, M.W., Bourdon, B., and Kleine, T., 2013, Experimental evidence for Mo  
535 isotope fractionation between metal and silicate liquids: *Earth and Planetary Science Letters*, v. 379, no. C, p.  
536 38–48.

537 Keays, R.R., 1995, The role of komatiitic and picritic magmatism and S-saturation in the formation of ore deposits:  
538 *Lithos*, v. 34, no. 1, p. 1–189.

539 Kerr, R. A. (1997). Deep-sinking slabs stir the mantle. *Science*, vol. 275, pp. 613-615.

540 Kleine, T., Touboul, M., Bourdon, B., Nimmo, F., Mezger, K., Palme, H., Jacobsen, S.B., Yin, Q.-Z., and Halliday,  
541 A.N., 2009, Hf–W chronology of the accretion and early evolution of asteroids and terrestrial planets:  
542 *Geochimica et Cosmochimica Acta*, v. 73, no. 17, p. 5150–5188.

543 Li, Y., and Audétat, A., 2012, Partitioning of V, Mn, Co, Ni, Cu, Zn, As, Mo, Ag, Sn, Sb, W, Au, Pb, and Bi  
544 between sulfide phases and hydrous basanite melt at upper mantle conditions: *Earth and Planetary Science*  
545 *Letters*, v. 355-356.

546 Mann, U., Frost, D.J., Rubie, D.C., Becker, H., and Audetat, A., 2012, Partitioning of Ru, Rh, Pd, Re, Ir and Pt  
547 between liquid metal and silicate at high pressures and high temperatures - Implications for the origin of highly  
548 siderophile element concentrations in the Earth's mantle: *Geochimica et Cosmochimica Acta*, v. 84.

549 McDonough, W.F., and Sun, S.S., 1995, The composition of the Earth: *Chemical Geology*, v. 120, no. 3, p. 223-  
550 253.

551 Nägler, T.F., Anbar, A.D., Archer, C., Goldberg, T., Gordon, G.W., Greber, N.D., Siebert, C., Sohrin, Y., and  
552 Vance, D., 2014, Proposal for an International Molybdenum Isotope Measurement Standard and Data  
553 Representation: *Geostandards and Geoanalytical Research*, v. 38, no. 2, p. 149-151.

554 Nisbet E.G., Cheadle M.J., Arndt N.T. and Bickle M.J., 1993, Constraining the potential temperature of the  
555 Archaean mantle: a review of the evidence from komatiites. *Lithos*, v. 30, no. 3-4, p. 291– 307.

556 Oze, C., Bird, D.K., and Fendorf, S., 2007, Genesis of hexavalent chromium from natural sources in soil and  
557 groundwater: *Proceedings of the National Academy of Sciences*, v. 104, no. 16.

558 Palme, H. and O'Neill, H.St.C., 2004, Cosmochemical estimates of Mantle Composition. In: *Treatise on*  
559 *Geochemistry*. Holland, H.D. and Turekian, K.K. (Editors), Elsevier, Amsterdam, The Netherlands. 2: 1-38.

560 Pearce, C.R., Cohen, A.S., Coe, A.L., and Burton, K.W., 2008, Molybdenum isotope evidence for global ocean  
561 anoxia coupled with perturbations to the carbon cycle during the Early Jurassic: *Geology*, v. 36, no. 3, p. 231.

562 Pettke, T., Oberli, F., Audetat, A., Guillong, M., Simon, A., Hanley, J., Klemm, L.M., 2012, Recent developments  
563 in element concentration and isotope ratio analysis of individual fluid inclusions by laser ablation single and  
564 multiple collector ICP-MS, *Ore Geological Reviews* 44, 10–38.

565 Puchtel, I.S., Blichert-Toft, J., Touboul, M., Walker, R.J., Byerly, G.R., Nisbet, E.G., and Anhaeusser, C.R., 2013,  
566 Insights into early Earth from Barberton komatiites: Evidence from lithophile isotope and trace element  
567 systematics: *Geochimica et Cosmochimica Acta*, v. 108, no. C, p. 63–90.

568 Puchtel, I.S., Haase, K.M., Hofmann, A.W., Chauvel, C., Kulikov, V.S., Garbe-Schonberg, C.D., and Nemchin,  
569 A.A., 1997, Petrology and geochemistry of crustally contaminated komatiitic basalts from the Vetryny Belt,  
570 southeastern Baltic Shield: Evidence for an early Proterozoic mantle plume beneath rifted Archean continental  
571 lithosphere: *Geochimica et Cosmochimica Acta*, v. 61, p. 1205–1222.

572 Puchtel, I.S., Humayun, M., Campbell, A.J., Sproule, R.A., and Leshner, C.M., 2004a, Platinum group element  
573 geochemistry of komatiites from the Alexo and Pyke Hill areas, Ontario, Canada: *Geochimica et*  
574 *Cosmochimica Acta*, v. 68, no. 6, p. 1361–1383.

575 Puchtel, I.S., Brandon, A.D., and Humayun, M., 2004b, Precise Pt–Re–Os isotope systematics of the mantle from  
576 2.7-Ga komatiites: *Earth and Planetary Science Letters*, v. 224, no. 1-2, p. 157–174.

577 Puchtel, I.S., Hofmann, A.W., Mezger, K., Shchipansky, A.A., Kulikov, V.S., and Kulikova, V.V., 1996, Petrology of  
578 a 2.41 Ga remarkably fresh komatiitic basalt lava lake in Lion Hills, central Vetryny Belt, Baltic Shield:  
579 *Contributions to Mineralogy and Petrology*, v. 124, p. 273–290.

580 Puchtel, I.S., Touboul, M., Walker, R.J., Blichert-Toft, J., Brandon, A.D., Kulikov, V.S., and Samsonov, A.V., (in  
581 prep). Lithophile and siderophile element systematics of the mantle at the Archean-Proterozoic boundary:  
582 Evidence from 2.4 Ga komatiites. *Geochimica et Cosmochimica Acta* (in preparation).

583 Puchtel, I.S., Walker, R.J., Touboul, M., Nisbet, E.G., and Byerly, G.R., 2014, Insights into early Earth from the Pt-  
584 Re-Os isotope and highly siderophile element abundance systematics of Barberton komatiites: *Geochimica et*  
585 *Cosmochimica Acta*, v. 125, no. C, p. 394–413.

586 Rudnick, R.L., and Gao, S., 2003, 3.01 - Composition of the Continental Crust: In *Treatise on Geochemistry*  
587 (Second Edition), eds. Holland, H.D., and Turekian, K.K., Elsevier, Oxford, v. 3, p. 1–64.

588 Rudge, J.F., Kleine, T., and Bourdon, B., 2010, Broad bounds on Earth's accretion and core formation  
589 constrained by geochemical models: *Nature Geoscience*, v. 3, no. 6, p. 439–443.

590 Siebert, J., Badro, J., Antonangeli, D., and Ryerson, F.J., 2013, Terrestrial Accretion Under Oxidizing Conditions:  
591 *Science*, v. 339, no. 6124, p. 1194–1197.

592 Stevenson, D.J., 2008, A planetary perspective on the deep Earth: *Nature*, v. 451, no. 7176, p. 261–265.

593 Van der Hilst, R. D. and Karason, H. (1999). Compositional heterogeneity in the bottom 1000 kilometers of Earth's  
594 mantle: Toward a hybrid convection model. *Science*, vol. 283, pp. 1885-1888.

595 Voegelin, A.R., Nägler, T.F., Pettke, T., Neubert, N., Steinmann, M., Pourret, O., and Villa, I.M., 2012, The impact  
596 of igneous bedrock weathering on the Mo isotopic composition of stream waters: Natural samples and  
597 laboratory experiments: *Geochimica et Cosmochimica Acta*, v. 86, p. 150–165.

598 Voegelin, A.R., Pettke, T., Greber, N.D., Niederhäusern, von, B., and Nägler, T.F., 2014, Magma differentiation  
599 fractionates Mo isotope ratios: Evidence from the Kos Plateau Tuff (Aegean Arc): *Lithos*, v. 190-191, p. 440–  
600 448.

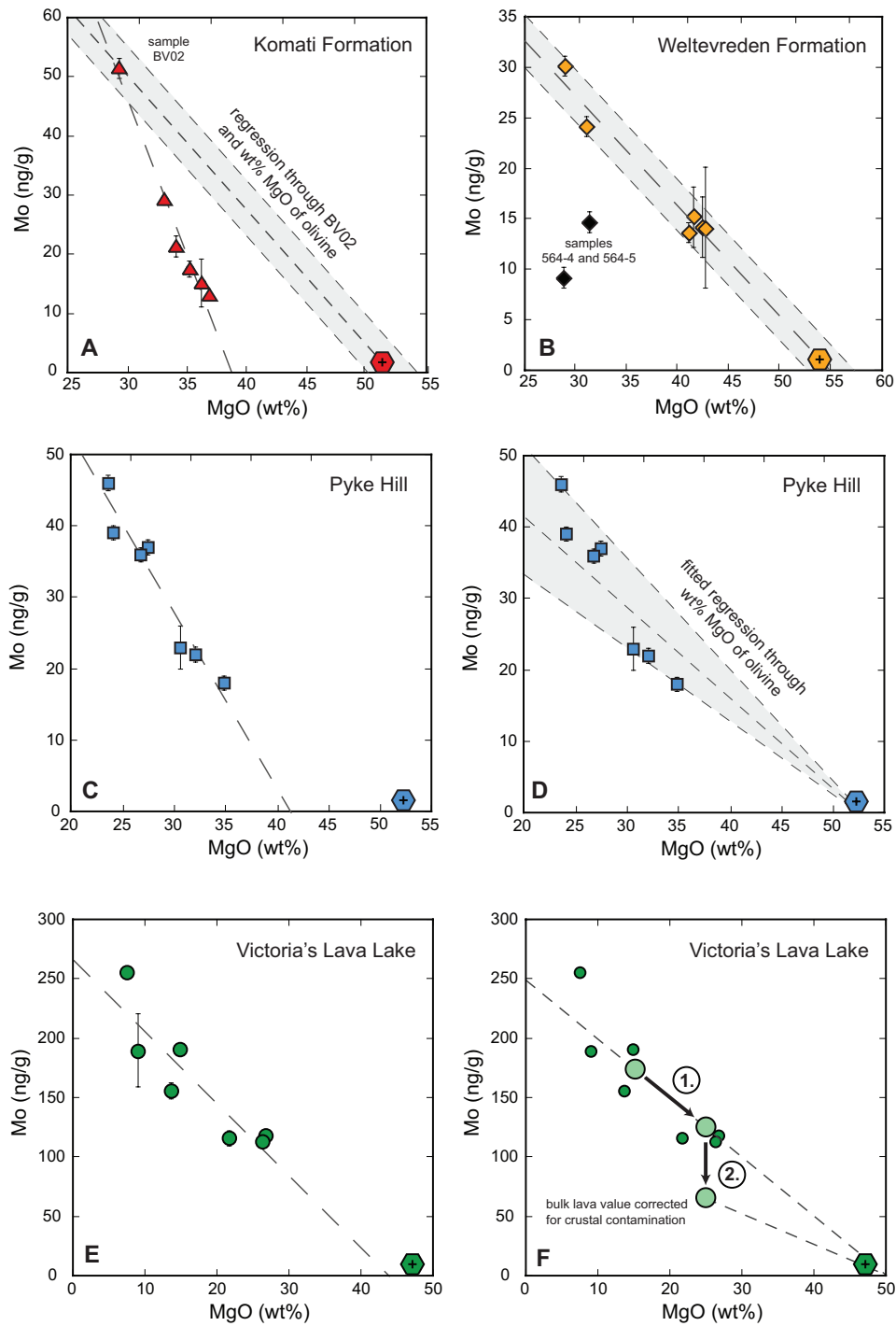
601 Wille, M., Kramers, J.D., Nägler, T.F., Beukes, N.J., Schröder, S., Meisel, T., Lacassie, J.P., and Voegelin, A.R.,  
602 2007, Evidence for a gradual rise of oxygen between 2.6 and 2.5 Ga from Mo isotopes and Re-PGE  
603 signatures in shales: *Geochimica et Cosmochimica Acta*, v. 71, p. 2417.

604 Wade, J., Wood, B.J., and Tuff, J., 2012, Metal-silicate partitioning of Mo and W at high pressures and  
605 temperatures: Evidence for late accretion of sulphur to the Earth: *Geochimica et Cosmochimica Acta*, v. 85.

606 Wood, B.J., Walter, M.J., and Wade, J., 2006, Accretion of the Earth and segregation of its core: *Nature*, v. 441,  
607 no. 7095, p. 825–833,

608

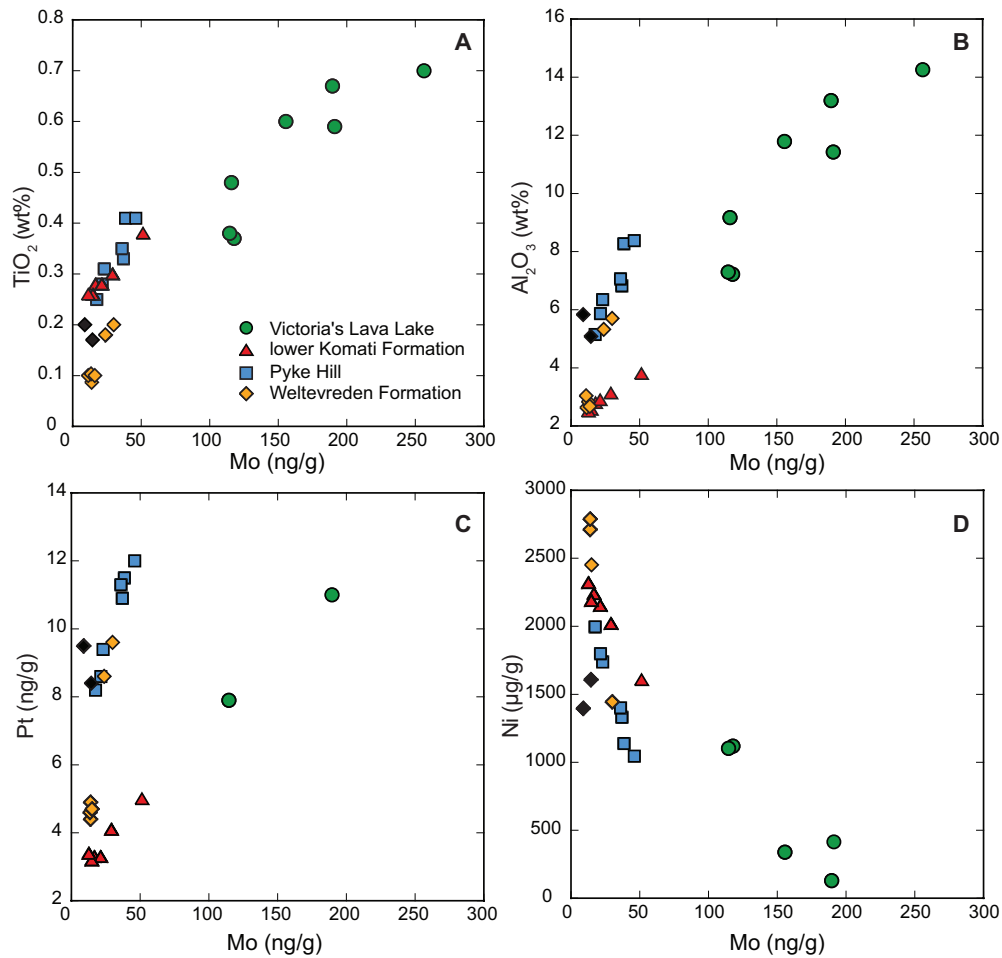
609 **Figures**



610

611 **Figure 1:** Variation diagrams of Mo vs. MgO for the investigated komatiite systems (A,B,C and E). Best estimates  
 612 of liquid lines of descents (A, D) and correction for crustal contamination (F) are indicated. For explanation of used  
 613 regressions (A, D) and different steps to correct for crustal contamination (F), see text. Samples 564-4 and 564-5  
 614 of the Weltevreden suite (B) have been omitted for liquid line of descent. Hexagons show the MgO concentration  
 615 of olivine from the literature. MgO concentrations of samples and olivine are from Puchtel et al. (1996, 2004a,  
 616 2013).

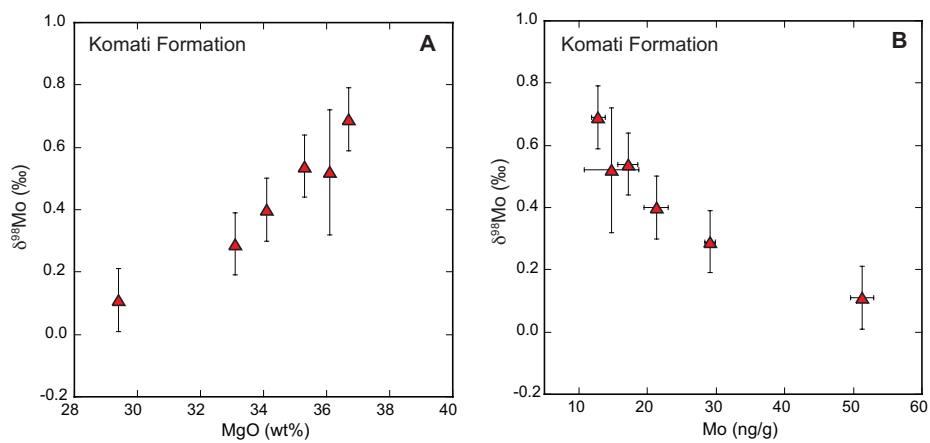
617



618

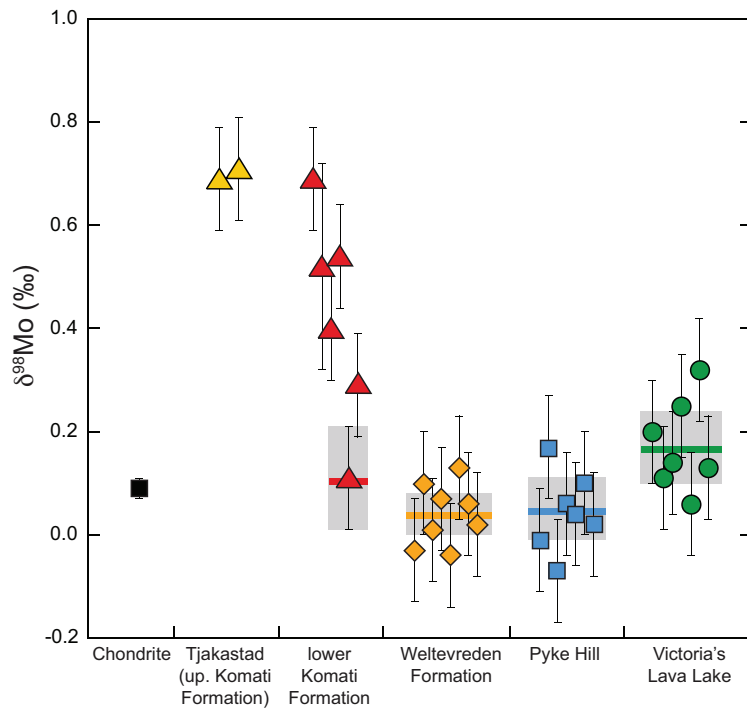
619 **Figure 2:** Variation diagrams for  $\text{TiO}_2$ ,  $\text{Al}_2\text{O}_3$ , Pt, and Ni vs Mo concentrations. Mo concentrations show positive  
 620 correlations with elements incompatible ( $\text{TiO}_2$ ,  $\text{Al}_2\text{O}_3$ , Pt) and negative with elements compatible (Ni) in olivine.  
 621 Major and trace element data are published in Puchtel et al. (1996, 2001, 2004a, 2013, 2014). Black Weltevreden  
 622 symbols are samples 564-4 and 564-5 that have been omitted for liquid line of descent (see Figure 1 and text).

623



624

625 **Figure 3:** Variation diagrams for  $\delta^{98}\text{Mo}$  vs. MgO (A) and Mo (B), for the lower Komati Formation komatiites only.  
 626 The Mo isotope compositions in these system correlate well with the MgO and the Mo concentrations and show  
 627 variation up to 0.60‰.



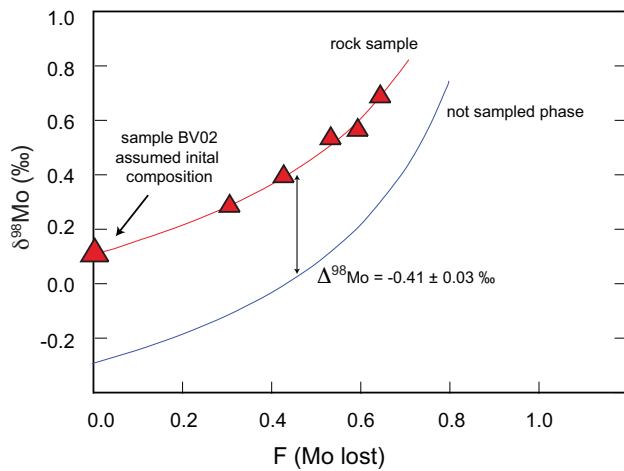
629

630 **Figure 4:** Summary of  $\delta^{98}\text{Mo}$  data. Colored lines with grey bars represent bulk Mo isotope composition of the  
 631 emplaced komatiite lavas. The Mo isotope composition of komatiites from Weltevreden, Pyke Hill and Victoria's  
 632 Lava Lake (not corrected for crustal contamination, see text) are very homogeneous and similar to the proposed  
 633 composition of enstatite and ordinary chondrites. The  $\delta^{98}\text{Mo}$  of the lower Komati Formation komatiites display a  
 634 large range with the most strongly altered samples from Tjakastad (upper Komati Formation) having the heaviest  
 635 Mo isotope composition. Errors on single measurements are 2SD of the standard reproducibility (i.e. 0.1‰, see  
 636 text). Errors on the displayed average data are 2SE except for Komati Formation (2SD on single measurement).  
 637  $\delta^{98}\text{Mo}$  of chondrite is from Burkhardt et al. (2014).

638



639



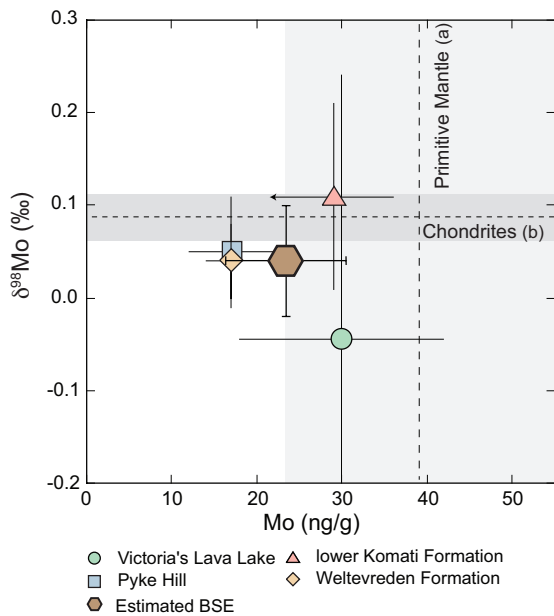
640

641 **Figure 5:** Modeled Rayleigh distillation for the Mo isotope variation among the lower Komati Formation, assuming

642 Mo loss after lava eruption for the samples that plot below the liquid line of descent indicated in Figure 1A. For

643 errors on  $\delta^{98}\text{Mo}$  see Figure 3 or Table 1.

644



645

646 **Figure 6:** Mo concentration of the komatiite mantle sources vs Mo isotope composition. Data is compared to

647 literature data (dotted lines = averages) and shows similarity between suggested Mo concentrations of the

648 primitive mantle (a: Palme and O'Neill 2004) and chondritic  $\delta^{98}\text{Mo}$  (b: Burkhardt et al., 2014). The arrow on the

649 error bar for sample from the lower Komati Formation indicates that its Mo concentration is a maximum estimate.

650 Mo signature for Victoria's Lava Lake is corrected for crustal contamination. Error calculations are described in the

651 text.

652

653 Table 1: Molybdenum concentration and isotope composition data

Sample	Location	Facies	$\delta^{98}\text{Mo}$ ‰				[Mo] ng/g			
			a	b	Average	2SD <sup>B</sup>	a	b	Average	2SD
01110/1		FB	0.09	0.17	0.13	0.10	193	190	191	4
01111		CM	0.29	0.35	0.32	0.10	158	153	156	7
91101		Sp	0.17	0.23	0.20	0.10	201	178	190	31
01001_A	Victoria's Lava Lake	OC	n.a	0.25	0.25	0.10	118	120	118	3
01105		OC	0.13	0.15	0.14	0.10	114	115	114	2
12124		Basalt	0.16	0.05	0.11	0.10	257	256	256	1
12106		OC	0.01	0.11	0.06	0.10	120	116	116	6
K04	Vodla Block	Tonalite	0.21	0.25	0.23	0.10	16	13	16	4
K13		Tonalite	-0.10	-0.05	-0.08	0.10	47	45	47	3
PH13		Sp	0.01	0.03	0.02	0.10	39	38	39	1
PH14		Sp	0.10	-	0.10	0.10	46	-	46	1
PH26		Sp	0.04	-	0.04	0.10	37	-	37	1
PH27	Pyke Hill	Sp	0.06	-	0.06	0.10	36	-	36	1
PH29		OC	-0.03	-0.10	-0.07	0.10	24	22	23	3
PH31		OC	0.19	0.15	0.17	0.10	17	18	18	1
PH33		OC	0.01	-0.03	-0.01	0.10	22	21	22	1
501-1		OC	n.a	0.02	0.02	0.10	16	12	14	6
501-3		Sp	n.a	0.06	0.06	0.10	24	24	24	1
501-8		OC	n.a	0.13	0.13	0.10	15	13	14	3
427-5	Weltevreden Formation	OC	n.a	-0.04	-0.04	0.10	14	13	14	1
564-4		Sp	0.07	n.a.	0.07	0.10	9	9	9	1
564-5		Sp	0.09	-0.08	0.01	0.10	15	14	15	1
12-2		Sp	0.10	-	0.10	0.10	30	-	30	1
12-7		OC	n.a	-0.03	-0.03	0.10	16	14	15	3
BV01		OC	0.37	0.22	0.29	0.10	29	29	29	1
BV02		CM	0.08	0.13	0.11	0.10	51	52	51	2
BV03	lower Komati Formation	OC	n.a	0.54	0.54	0.10	17	18	17	1
BV10		OC	0.38	0.41	0.4	0.10	22	21	21	2
BV13 <sup>A</sup>		OC	0.66	0.37	0.52	0.20	13	16	15	4
BV15		OC	0.71	0.68	0.69	0.10	13	12	13	1
Tjakastad-1	upper Komati Formation	Sp	0.73	0.69	0.71	0.10	81	83	82	3
Tjakastad-2		Sp	0.69	-	0.69	0.10	81	-	81	2
SDO-1	USGS Rock standard		1.07 ± 0.05 (2SD; n=5)							

654 Facies: FB= flow top breccia; CM= chilled margin; Sp= spinifex; OC= olivine cumulate

655 A: Not reproduced sample, 2SD of  $\delta^{98}\text{Mo}$  longterm reproducibility is doubled656 B:  $\delta^{98}\text{Mo}$  reproducibility of reference standard  $\leq \pm 0.10\%$  (2SD) see text and Greber et al., (2012)657 Mo concentrations are recalculated on an anhydrous basis using LOI from literature (Puchtel et al., 1996; Puchtel et al., 2004a;  
658 Puchtel et al., 2013)659 Accuracy of single Mo ID concentration measurements is  $\pm 2\%$  (Greber et al., 2012) and is applied for samples that were  
660 measured only once

661 n.a: not available due to wrong sample-spike ratio or too low Mo signal

662

663 Table 2: Summary of estimated Mo concentrations and isotope compositions of emplaced komatiites,  
 664 mantel sources and the Bulk Silicate Earth

	Mo (ng/g)		$\delta^{98}\text{Mo}$ (‰)
	Emplaced lava	Mantle source	
Victoria's Lava Lake <sup>A</sup>	66 ± 22	30 ± 12	-0.04 ± 0.28
Pyke Hill	33 ± 8	17 ± 5	0.05 ± 0.06
Weltevreden	25 ± 4	17 ± 3	0.04 ± 0.04
lower Komati Formation	51 ± 6	29 ± 7	0.11 ± 0.10
<b>Estimated BSE <sup>B</sup></b>		<b>23 ± 7</b>	<b>0.04 ± 0.06</b>

665 A: Corrected for crustal contamination (see text)

666 B: Errors are 2SE

667